Using a Liquid Xenon Positron Target

Max Varverakis* and Robert Holtzapple†
California Polytechnic State University, San Luis Obispo, CA 93407, USA

Spencer Gessner‡
SLAC National Accelerator Laboratory, Menlo Park, California 94025, USA

Hiroki Fujii§
Nishina Center, RIKEN, 2-1 Hirosawa, Wako, Saitama, 351-0198, Japan
(Dated: August 17, 2022)

Positron targets are a critical component of future Linear Colliders. Traditional targets are composed of high-Z metals and become brittle over time due to constant bombardment by high-power electron beams. We explore the possibility of a liquid Xenon target which is constantly refreshed and therefore not susceptible to the damage mechanisms of traditional solid targets. Using the GEANT4 simulation code, we examine the performance of the liquid Xenon target and show that the positron yield and divergence are comparable to solid targets when normalizing by radiation length. We develop parameter sets for a demonstration application at FACET-II and an ILC-type positron source.

I. INTRODUCTION

For future Linear Collider applications, around 10^{14} e^+ per second need to be produced [1]. In addition to the quantity of positrons, they generally need to have a minimum energy based off of the design of the accelerator.

The traditional scheme for producing positrons is by colliding high energy electrons into a high-Z target. The collision between an electron beam and a target generates an electromagnetic particle shower producing positrons.

In order to generate 10^{14} e^+ per second, an extremely high-powered electron beam is required, which results in a large power deposited in the target. Hence, solid targets tend to degrade over time [2].

Previous experiments have been carried out to explore alternatives to using solid targets, such as using liquid Mercury (Hg), but the apparent hazards that Hg presents are too dangerous to implement in any efficient manner [3]. Other liquid targets have been investigated in the undulator scheme for ILC, such as Bi-Pb [3] and Pb [4]. Related studies include using liquid Lithium to generate neutrons from a proton beam [5], as well as using a gaseous deuterium target and positron beam for muon production [6].

In this paper, we explore the use of a liquid Xenon (LXe) target to produce positrons under the hypothesis that the liquid flow will be able to account for the power deposits discussed above. Figure 1, a basic schematic of the liquid Xenon target and beam interaction.

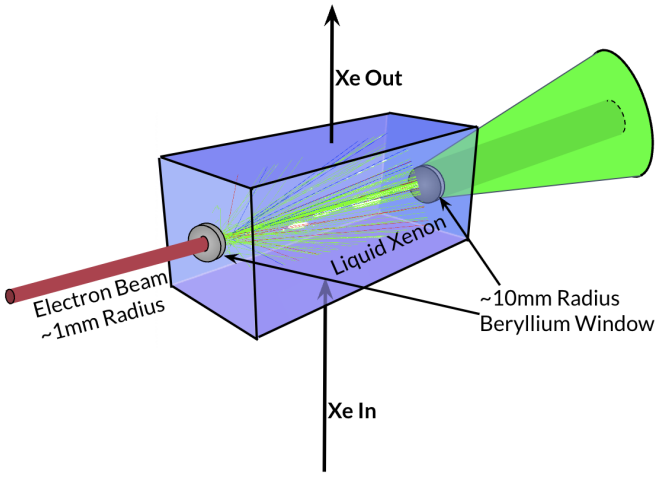

FIG. 1: Liquid Xenon target setup.

II. SIMULATION RESULTS

Using GEANT4 [7], we compare our liquid Xenon target to a Tantalum target due to previous experience with Tantalum positron targets at FACET-II [8]. We expect to see similar positron yields for both targets when normalizing by radiation lengths. Since the radiation length of liquid Xenon is around 7 times greater than that of Tantalum, the the transverse spread of the positron shower should be larger in the liquid Xenon target. For practical purposes, other than for energy deposition considerations, we do not consider positrons on the exit of the target under 20 MeV and over 10 mm transverse displacement, which is based off of similar positron energy acceptances in [9][10]. See Table I for parameters used in the simulation.

To calculate the RMS emittance of the positrons generated in pair production, we utilize the following [11]

* mvarvera@calpoly.edu
† rholtzap@calpoly.edu
‡ sgess@slac.stanford.edu
§ hiroki.fujii@riken.jp

Material	Symbol	Z	Density [$g \cdot cm^{-3}$]	Rad Length [cm]
Tantalum	Ta	73	16.654	0.4094
Liquid Xe	LXe	54	2.953	2.872

TABLE I: Parameters used in GEANT4 simulation when comparing targets.

$$\varepsilon_{n,rms} = \frac{1}{m_0 c}\sqrt{\langle x^2\rangle \langle p_x^2\rangle - \langle x p_x\rangle}. \quad (1)$$

Using these equations, we calculate the RMS emittance of the positrons for both Tantalum and liquid Xenon targets. At max positron yield, the transverse emittance for Ta is $\sim 9\text{mm} \cdot \text{rad}$ while the transverse emittance for LXe is $\sim 56\text{mm} \cdot \text{rad}$. According to [10], the transverse emittance for liquid Xenon is comparable for use in linear colliders.

From Figure 2, the max positron yield for both Ta and LXe occurs at around 4.5 radiation lengths. Despite having different radiation lengths, the energy of the positrons exiting the target at a given width are relatively equal for both target materials.

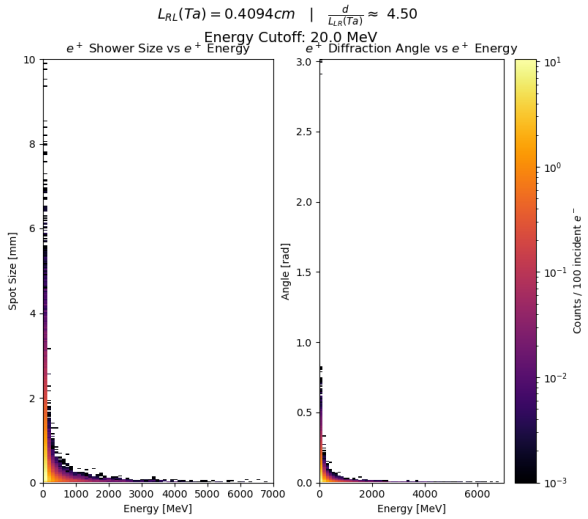

(a) Tantalum target.

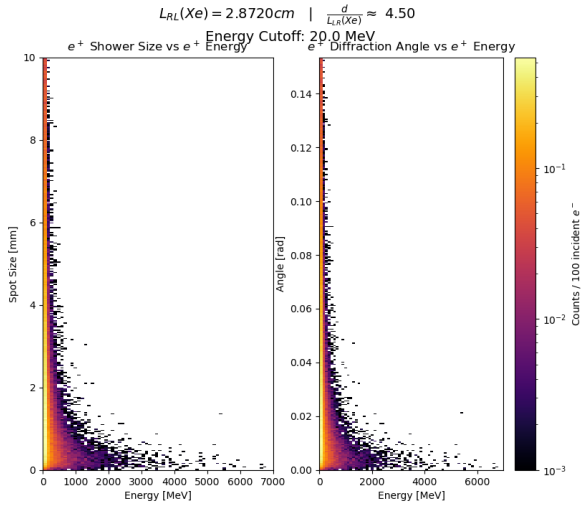

(b) Liquid Xenon target.

FIG. 3: Traverse width and angular diffraction of positrons as a function of their energy upon target exit. Data is shown for widths of 5.5 radiation lengths (max e^+ yield).

Notice that in Figure 3, the angular divergence of positrons is roughly the same for both targets, yet the traverse widths are more broadly distributed for the liquid Xenon target. This can be explained by the fact that the radiation length of LXe is roughly seven times that of Tantalum.

In simulation, we compare the energy deposited in the target for both materials per incident e^-. Although these deposits seem quite high, as we indicate in Section III A, the flow of LXe can take into account the energy deposit without much concern.

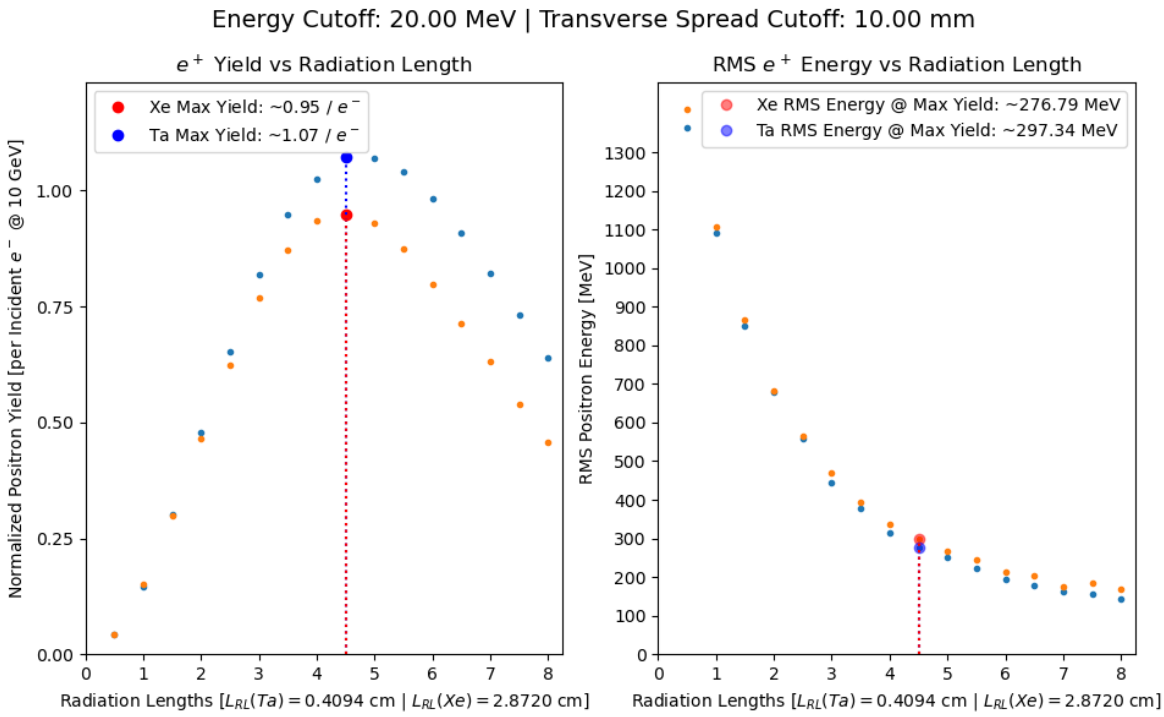

FIG. 2: Positron yield and RMS energy upon exiting the target per incident e^- at 10 GeV.

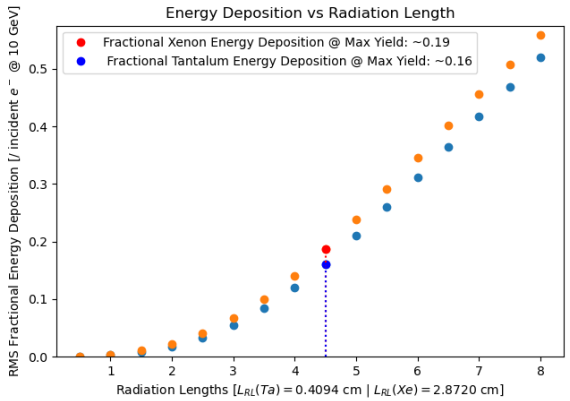

FIG. 4: Energy deposition in Ta and LXe targets per incident electron at 10 GeV.

It is reassuring to see that even after removing the positrons from the dataset with large transverse distances from the beam path, there are still a comparable number of positrons that we predict will be able to make it to the next stage of the accelerator [].

III. CRYO-COOLED LIQUID XENON CHAMBER

A. Calculating the Liquid Xenon Flow Rate

To calculate the flow rate of the liquid Xenon, we first calculate preliminary values using the information given in the table below. To see resultant quantities, seek Table III.

Liquid Xenon	Symbol	Value	Units
Molar Mass	M	131.293	u
Density	ρ	2.953	$g \cdot cm^{-3}$
Vapor Pressure	p	300	kPa
Heat of Vaporization	ΔH	12.636	$kJ \cdot mol^{-1}$
Heat of Vap./Volume	ΔH_{vol}	284.205	$J \cdot cm^{-3}$
Radiation Length	L_{RL}	2.872	cm
Width	$\frac{d}{L_{RL}}$	4.5	L_{RL}

TABLE II: Important parameters associated with liquid Xenon target chamber.

We first convert the heat of vaporization to units of Joules per unit volume ($J \cdot cm^{-3}$), which is given by Eq. (2a). Then, one can calculate the number of electrons per beam bunch, by comparing the total charge of the beam bunch to the charge of an electron ($e \approx 1.602 \times 10^{-10}$ nC), as follows from Eq. (2b). From this, we calculate the total energy deposited in the liquid Xenon

Beam Parameters	**Symbol**	**FACET-II** [12]	**ILC** [1]	**Units**
Energy	E	10.0	6.0	GeV
Repetition Rate	f	10	300	Hz
Charge	q	2	3.204	nC
Number of e^-	n	1.248	2.0	10^{10}
Resultant Quantities				
Energy Deposition/e^-	$\mathrm{E_{dep}}$	1.9		GeV
Energy Deposit/Pulse	ϵ	3.8	482.1	J
Peak Energy Deposit Density	ϵ_ρ	1.96×10^{-2}	15.22	$\mathrm{J{\cdot}g^{-1}}$
Power Deposit/Pulse	P_{dep}	38.0	1.45×10^5	W
Flow Rate due to Vaporization	Q	0.134	508.9	$\mathrm{cm^3 \cdot s^{-1}}$
Main Shower Path Flow Rate	Q_{vol}	0.5170	15.51	$\mathrm{L{\cdot}s^{-1}}$

TABLE III: Linear collider electron beam parameters and associated target quantities.

target, as seen in Eq. (2c).

$$\Delta \mathrm{H_{vol}} = \frac{\Delta \mathrm{H} \cdot \rho}{\mathrm{M}}, \tag{2a}$$

$$n = \frac{q}{e}, \tag{2b}$$

$$\epsilon = n \cdot E_{\mathrm{dep}}. \tag{2c}$$

We can obtain the flow rate of liquid Xenon required to replace the vaporized Xenon due to the energy deposited by the beam,

$$Q = \frac{\epsilon \cdot f}{\Delta \mathrm{H_{vol}}}. \tag{3}$$

In case one wants to calculate the flow rate required to move the entire volume encompassing the main part of the EM shower, one can approximate the volume with a rectangular prism with target width and other side lengths equal to the diameter of the Beryllium windows (see next section). At max positron yield, this gives $\mathrm{V} = (2\ \mathrm{cm})^2 \cdot 4.5\mathrm{L_{RL}} \approx 51.70\ \mathrm{cm}^3$. As a result, the required flow rate to move volume V in the amount of time between beam pulses is shown in Table III as Q_{vol}.

B. Using Beryllium Windows to the Target Chamber

We explore using Beryllium windows for the beam to enter and exit the target chamber.

Beryllium	**Symbol**	**Value**	**Units**
Atomic Number	Z	4	
Density	ρ	1.844	$\mathrm{g{\cdot}cm^{-3}}$
Rupture Modulus	F_a	400	MPa
Quantities			
Height	h	1.0	m
Radius	r	10.00	mm
Contact Area	A	100π	$\mathrm{mm^2}$
Pressure	P	328.968	kPa
Force	F	9.100	N
Safety Factor	S_F	4	
Empirical Constant	K	0.75	
Thickness	T	147.395	μm

TABLE IV: Useful quantities and properties of solid Beryllium. The quantities are specific to a 10mm radius Beryllium disk [?].

Utilizing Bernoulli's Equation for conservative force fields [], we can calculate the total pressure on a Beryllium window, which is of the form

$$P = \frac{1}{2}\rho v^2 + \rho g h + p, \tag{4}$$

where v is the fluid flow rate, g is acceleration due to gravity, h is the height of the Xenon chamber relative to the height of the window, and p is the additional external pressure (in this case p refers to the vapor pressure of LXe $\sim$ 300kPa). However, as seen in Table III, the flow rate for the liquid Xenon is quite small. Therefore, we can ignore the second order term to further simplify our approximation to

$$P = \rho g h + p. \tag{5}$$

From Eq. (5), we can calculate the force on a Beryllium window with contact area A by multiplying the area by the pressure: $F = P \cdot A$.

In order to determine the required thickness of the Beryllium window, we utilize the following [13]. First we calculate a constant related to the safety factor of our thickness, which takes into account the method with which the Beryllium window is inserted into the target

chamber. An empirical constant $K = 0.75$ is chosen if the window is clamped into the target chamber, and $K = 1.125$ if the window is unclamped in the target chamber. For a given safety factor (S_F), we have a thickness of

$$T = r \cdot \sqrt{\frac{S_F \cdot K \cdot P}{F_a}}. \tag{6}$$

For parameters chosen in Table IV, we get a required thickness of 496.701μm. Using the above thickness, we simulated the energy deposited in both of the Beryllium windows, and found that the energy deposited in the entrance window is on the order of 10^{-1} MeV/incident e^- and the exit window on the order of 6 MeV/incident e^-.

TODO Explore how much heat Be windows can take in given amount of time like done above for LXe??

IV. CONCLUSION

A. Design of Liquid Xenon Chamber

Here we explore how one could design a chamber for the liquid Xenon target.

Source code and sample data from GEANT4 simulations can be found at `https://github.com/MaxVarverakis/LiquidXenonSims.git`.

[1] Y. Seimiya, M. Kuriki, T. Takahashi, T. Omori, T. Okugi, M. Satoh, J. Urakawa, and S. Kashiwagi, Positron capture simulation for the ILC electron-driven positron source, Progress of Theoretical and Experimental Physics **2015**, 103G01 (2015).

[2] V. Bharadwaj, Y. Batygin, J. Sheppard, D. Schultz, S. Bodenstein, J. Gallegos, R. Gonzales, J. Ledbetter, M. Lopez, R. Romero, T. Romero, R. Rutherford, and S. Maloy, Analysis of beam-induced damage to the slc positron production target, in *PACS2001. Proceedings of the 2001 Particle Accelerator Conference (Cat. No.01CH37268)*, Vol. 3 (2001) pp. 2123–2125 vol.3.

[3] A. A. Mikhailichenko, Liquid metal target for ilc, in *Proceedings of EPAC 2006, Edinburgh, Scotland* (2006).

[4] J. C. Sheppard, *Liquid Metal Target for NLC Positron Source*, Tech. Rep. (2002).

[5] G. Feinberg, M. Paul, A. Arenshtam, D. Berkovits, Y. Eisen, M. Friedman, S. Halfon, D. Kijel, A. Nagler, A. Shor, and I. Silverman, A liquid-lithium target project for production of high-intensity quasi-stellar neutrons, in *Proceedings of 11th Symposium on Nuclei in the Cosmos — PoS(NIC XI)* (Sissa Medialab, 2011).

[6] H. Okita, Y. Ishi, and Y. Mori, Beam emittance growth in the proposed gaseous target ERIT ring for muon production, Nuclear Instruments and Methods in Physics Research Section A: Accelerators, Spectrometers, Detectors and Associated Equipment **982**, 164565 (2020).

[7] S. Agostinelli *et al.* (GEANT4), GEANT4–a simulation toolkit, Nucl. Instrum. Meth. A **506**, 250 (2003).

[8] H. Fujii, K. Marsh, W. An, S. Corde, M. Hogan, V. Yakimenko, and C. Joshi, Positron beam extraction from an electron-beam-driven plasma wakefield accelerator, Physical Review Accelerators and Beams **22**, 10.1103/physrevaccelbeams.22.091301 (2019).

[9] H. Tang, A. Kulikov, J. Clendenin, S. Ecklund, R. Miller, and A. Yeremian, The NLC positron source, in *Proceedings Particle Accelerator Conference* (IEEE, 1995).

[10] J. Sheppard, *Conventional Positron Target for a Tesla Formatted Beam(LCC-0133)*, Tech. Rep. (2003).

[11] K. Floettmann, Some basic features of the beam emittance, Physical Review Special Topics - Accelerators and Beams **6**, 10.1103/physrevstab.6.034202 (2003).

[12] N. G. Author, *Technical Design Report for the FACET-II Project at SLAC National Accelerator Laboratory*, Tech. Rep. (2016).

[13] C. Ltd, *The CRYSTRAN HANDBOOK of Infra-Red and Ultra-Violet OPTICAL MATERIALS* (Crystran Ltd, 2019).